

Quantum-limited Mixing in a Transformer-coupled SIS Resonator for the 600 GHz Frequency Band

Cheuk-yu Edward Tong, Raymond Blundell

Harvard-Smithsonian Center for Astrophysics, 60 Garden Street, Cambridge, MA 02138.

Krikor G. Megerian, Jeffrey A. Stern, Henry G. LeDuc

Jet Propulsion Lab, California Institute of Technology, 4800 Oak Grove Drive, Pasadena, CA 91109.

Abstract

Quantum-limited mixer noise temperature has been achieved in Superconductor-Insulator-Superconductor (SIS) resonant mixer in the 600 – 720 GHz frequency range. Our mixer employs a single full-wave Nb/AlN/Nb tunnel junction resonator, fed by a quarter-wave transformer. The devices have low critical current density ($\sim 5 \text{ kA/cm}^2$). The mixers were tested in a fixed-tuned waveguide mixer mount. Double-side-band receiver noise temperatures equivalent to a few quanta have been measured for a number of different devices. Using a $0.55 \times 25 \mu\text{m}$ resonator, a noise temperature of 141 K was recorded at an LO frequency of 700 GHz with the mixer at 4.2 K. The noise temperature dropped to 111 K when the helium bath was pumped down to 2.8 K. High sensitivity has attained over reasonably wide RF bandwidth, $\sim 17\%$. The IF bandwidth of these mixers has also been investigated.

I. Introduction

The introduction of distributed mixing in Superconductor-Insulator-Superconductor (SIS) junctions is an important development in low-noise receiver technology for sub-millimeter wavelengths [1,2]. The earliest distributed mixers employed fairly long superconducting tunnel junctions, about 2 wavelengths long. The long junction acts as a lossy transmission line in which mixing occurs along the whole length of the line. This class of receiver has demonstrated sensitivities close to the quantum limit. A noise temperature of

$3hv/k$ was recorded at 460 GHz [1], where hv is the photon energy and k is the Boltzmann constant.

In a subsequent development, Belitsky [3] proposed that distributed mixing could also be implemented in SIS resonators. One advantage of resonant distributed mixing is that the resonator can achieve a higher impedance level compared to simple long superconducting transmission lines which generally have very low characteristic impedance. Uzawa [4] performed experiments with resonant distributed mixers incorporating a niobium nitride SIS resonator in the 800 GHz frequency band. Finally, in 2001, Matsunaga [5] implemented distributed mixing using dual SIS resonators connected in series through impedance transformers, employing standard Nb/Al/AlOx/Nb SIS junctions fabricated with optical lithography. That mixer exhibited high sensitivity, with a measured noise temperature of 185 K at 630 GHz.

Following this encouraging result, we have developed resonant mixers based on Nb/AlN/Nb junctions fabricated with electron-beam lithography at Jet Propulsion Lab. In this paper, we demonstrate that the sensitivity of $0.6 \mu\text{m}$ wide full-wave SIS resonators can reach quantum-limited performance in the 600 GHz band, at frequencies that approach the band gap frequency of niobium.

II. Modeling of the SIS Resonator

Fig. 1 shows the cross-section of the SIS non-linear transmission line, which reduces to a simple microstrip line when the width of the tunnel barrier, W_j , is zero. Such a linear superconducting microstrip line can readily be modeled by various approaches. We have employed the analysis described in [6], using frequency dependent surface impedances from the Mattis-Bardeen Theory [7]. Let Z_0 and γ_0 be the characteristic impedance and complex propagation constant of the line respectively for $W_j = 0$. If W_j is much smaller than the width of top conductor of the microstrip, W_s , we can write down the per unit length series impedance of the

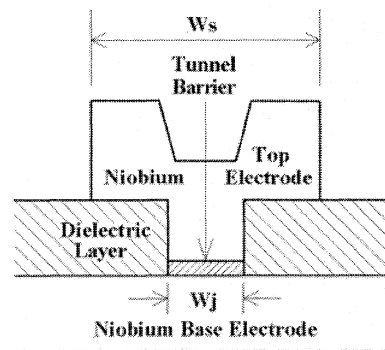


Fig. 1 Cross-sectional view of an SIS non-linear transmission line. In our mixers, the tunnel barrier is Aluminum Nitride (AlN) and the dielectric layer is 250 nm thick of Silicon Oxide (SiO). The width of the wiring layer, W_s , is $4 \mu\text{m}$.

transmission line as:

$$Z_s = \gamma_0 Z_0 (1 - W_j / W_s), \quad (1)$$

and the per unit length parallel admittance as:

$$Y_p = \frac{\gamma_0}{Z_0} \left(1 - \frac{W_j}{W_s}\right) + j\omega C_{sp} W_j + \xi \frac{W_j}{R_N A} \quad (2)$$

where C_{sp} is the specific capacitance of the tunnel junction per unit area, $R_N A$ is the product of normal state resistance and area of the junction and ξ is a signal mixing factor. In equation (2), the second term represents the contribution of the geometrical capacitance of the tunnel junction and the third term represents the mixing conductance due to the tunneling quasiparticle current, G_{qp} [3].

From Tucker's quantum theory of mixing [8], we can write down an expression for ξ :

$$\xi = G_{qp} R_N = \frac{e R_N}{2 h \nu} \cdot \sum_{n=-\infty}^{\infty} [J_{n-1}^2(\alpha) - J_{n+1}^2(\alpha)] I_{dc} \left(V_0 + \frac{n h \nu}{e} \right) \quad (3)$$

where $\alpha = e V_{LO} / h \nu$ is the normalized voltage impressed by the Local Oscillator (LO) across the junction, $I_{dc}(V)$ is the DC current-voltage characteristic of the junction and V_0 is the DC bias voltage at the operating point. From our simulation, we find that a niobium based SIS resonator should operate well with $\alpha \sim 0.7$ and $V_0 \sim 1.5$ mV for $\nu \sim 660$ GHz. Under these conditions, equation (3) gives $\xi \sim 0.8$. By assigning a constant value to ξ , we assume that the distributed mixer may be described by a linear model [1].

Once Z_s and Y_p are known, we can evaluate the key parameters of the non-linear transmission line, including the characteristic impedance, Z_c , the complex propagation constant, γ , and the guided wavelength, λ_g .

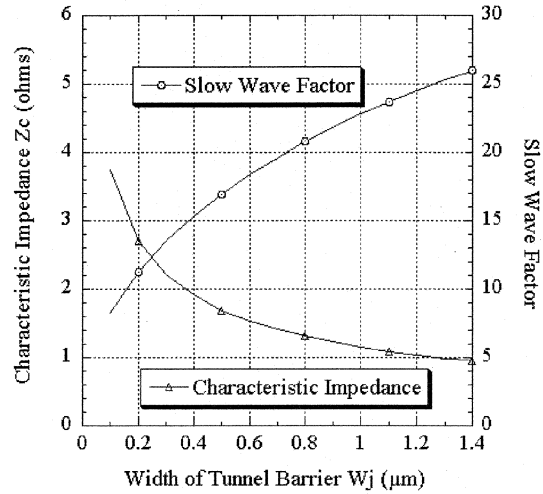


Fig. 2 Variation of Characteristic Impedance, Z_c , and Slow Wave Factor, λ_0 / λ_g , as a function of W_j for our mixers at a frequency of 660 GHz. We have taken $W_s = 4 \mu\text{m}$, $C_j = 65 \text{ fF}/\mu\text{m}^2$ and $R_N A = 40 \mu\text{m}^2$.

$$Z_c = Z_s / Y_p \quad (4)$$

$$\gamma = \sqrt{Z_s \cdot Y_p} \quad (5)$$

$$\lambda_g = \frac{\lambda_0}{2\pi} \cdot \text{Im}(\gamma) \quad (6)$$

The characteristic impedance and the slow wave factor, λ_0/λ_g , for our mixer as a function of the width of the tunnel barrier, W_j , are plotted in Fig. 2. From the figure, it can be seen that Z_c is not a strong function of W_j for $W_j > 0.4 \mu\text{m}$. However, λ_g is strongly dependent on the width of the tunnel junction.

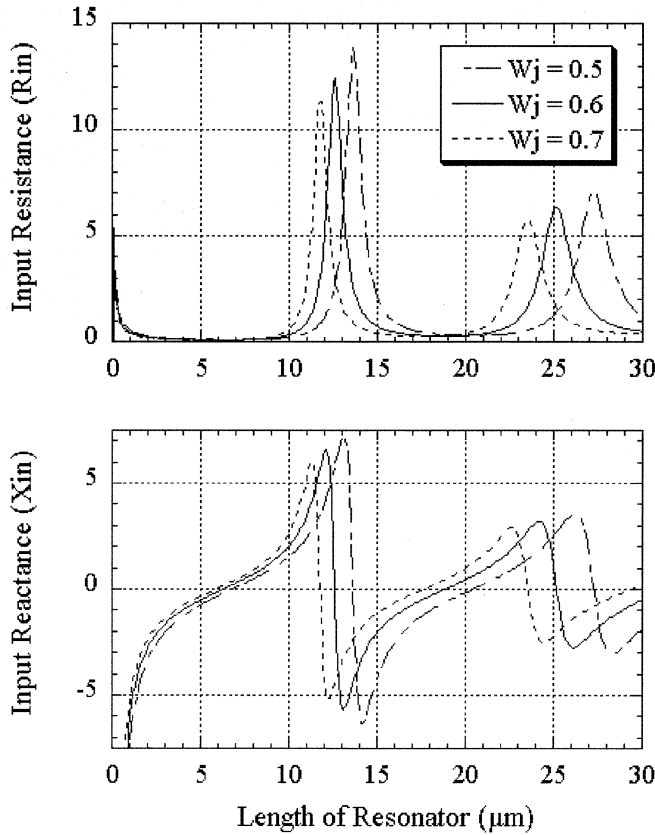


Fig. 3 Input impedance of SIS Resonator at 660 GHz as a function of resonator length for $W_j = 0.5, 0.6$ and $0.7 \mu\text{m}$. R_{in} is the real part and X_{in} is the imaginary part of the input impedance, where $R_{\text{in}} + j X_{\text{in}} = Z_c(W_j) \cdot \coth(\gamma(W_j) \cdot L_j)$ and L_j is the length of the resonator.

In fig. 3 we display the input impedances of 3 SIS resonators with different junction widths. The length for half-wave resonance is about $12 \mu\text{m}$ and full-wave resonance occurs around $25 \mu\text{m}$. As discussed above, the resonant impedance level is not a strong function of W_j . However, for a given length of resonator, the resonant frequency is quite sensitive to the junction width.

In our experiments, we have chosen to work with full-wave resonators rather than half-wave resonators because the value of dX_{in}/df is smaller at full-wave resonance, hence a larger impedance bandwidth can be achieved.

III. Mixer and Receiver Design

In order to match the low input resistance ($\sim 6 \Omega$) at the full-wave resonance of the non-linear SIS resonator, we use a $3 \mu\text{m}$ wide niobium microstrip transformer section to couple the signal power from our fixed-tuned waveguide mixer mount [9,10]. The layout of the center of the mixer chip is shown in Fig. 4. Since the resonant frequency is highly dependent on the exact width of the junction, we have fabricated chips with different junction widths and lengths about the nominal dimensions of $0.6 \times 25 \mu\text{m}$. We had a target current density of $5 \text{ kA}/\text{cm}^2$, which corresponds to $R_{NA} = 40 \Omega \mu\text{m}^2$.

The mixer is tested in a laboratory test dewar, the details of which have been described elsewhere [5,11]. In all the experiments, we have used an IF center frequency of 3 GHz and the signal and LO input to the dewar are combined using a wire grid polarizer as a beam splitter in front of the cryostat vacuum window. The receiver IF output is measured by a power meter, over the band 2.4 – 3.6 GHz. Fig. 5 shows a photo of the set-up of our measurement bench.

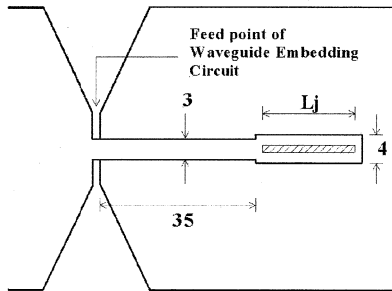


Fig. 4 Line drawing of mixer chip layout, showing the microstrip transformer section and the SIS resonator. The drawing is not to scale and the dimensions are in μm .

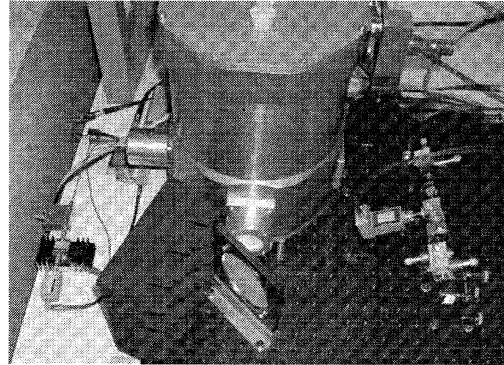


Fig. 5 Set-up of laboratory receiver measurement. LO unit is located on the right. The LO beam is focused by a 90° parabolic mirror and is injected into the dewar by a wire grid polarizer. The 3 GHz room temperature IF chain is on the left.

IV. Receiver Performance

The receiver noise temperature was measured using the standard Y-factor method with ambient (295 K) and liquid-nitrogen cooled (77 K) loads.

We have tested a number of different mixer chips, and fig. 6 shows the current-voltage

and power-voltage characteristics of a $0.55 \times 25 \mu\text{m}$ resonator, and the variation of Y-factor with bias voltage, when driven by a 700 GHz LO. The gap voltage is 2.85 mV at a bath temperature of 4.2 K. The mixer is, therefore, operating close to its gap frequency of 690 GHz. The tunneling current at 4 mV bias is about 1.4 mA, which corresponds to a normal state resistance of about 2.8Ω . The sub-gap leakage current at 2 mV bias is about $66 \mu\text{A}$, which corresponds to a sub-gap leakage resistance of about 31Ω . A small magnetic field is applied so that the IF power output is minimized at 1.45 mV bias, where the first Shapiro step occurs.

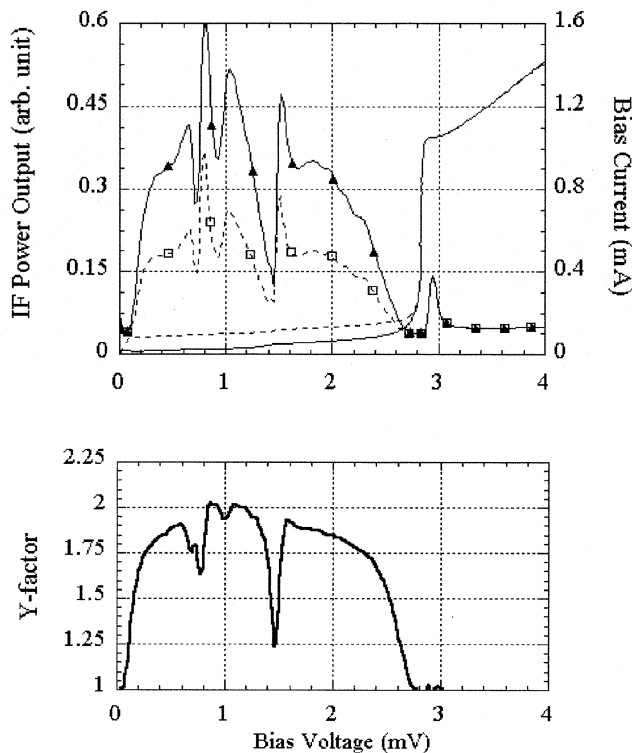


Fig 6 The top figure shows the Current Voltage Characteristics of a $0.55 \times 25 \mu\text{m}$ resonant mixer without LO (solid line) and in the presence of LO power at 700 GHz (dotted line). On the same figure, the receiver IF power output is also displayed. The solid line with markers \blacktriangle gives the response to a 295 K load, and the dotted line with markers \square gives the response to a 77 K load. The bottom figure shows the variation of Y-factor as a function of bias voltage. The bath temperature was 4.2 K.

A Y-factor of 2 was observed at a bias setting of 1.1 mV and 0.1 mA, corresponding to a double-side-band (DSB) Rayleigh-Jean noise temperature of 141 K. In spite of the high value of dP_{out}/dV at this bias setting, the receiver was found to be very stable. The estimated DSB conversion loss was about 7.5 dB. At a bias of 1.7 mV, the Y-factor was 1.92, improving to 1.95 when the LO power was slightly increased. The Y-factor showed a dip at a bias of 0.75 mV. We believe that this was caused by Josephson oscillation at about 360 GHz, the frequency at which the mixer becomes a half-wave resonator.

When the helium bath temperature was reduced to 2.8 K, the sub-gap leakage current decreased to $54 \mu\text{A}$. Conversion loss was decreased by about 1 dB and the Y-factor measured at

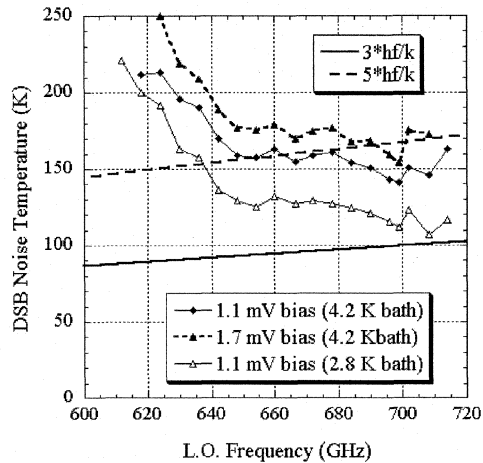


Fig. 7 Noise temperature of 0.55x25 μm SIS resonator as a function of L.O. frequency. Noise temperature is calculated from measured Y-factor in the Rayleigh-Jeans regime, by $T_n = (295-77Y)/(Y-1)$.

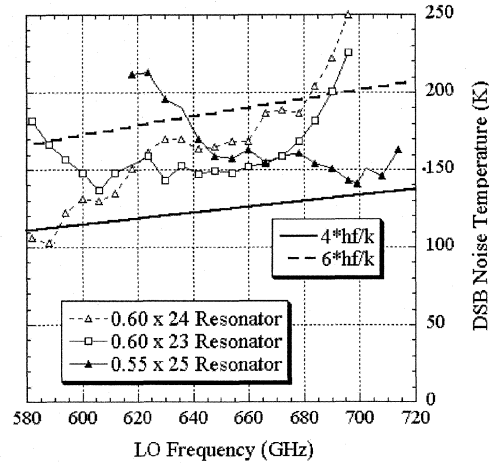


Fig. 8 Performance of different mixers biased at 1.1 mV with a 4.2 K helium bath. Also shown are the noise temperature corresponding to 4 and 6 photons.

1.1 mV bias point jumped to 2.16, corresponding to a DSB Rayleigh-Jean noise temperature of 111 K. This noise temperature is equivalent to $3.3 \, h\nu/k$, which implies that the sensitivity is quantum-limited. The decrease in receiver noise temperature of about 30 K is mainly due to a reduction of leakage current. The gap voltage only changed by 0.05 mV and should only have a small impact on sensitivity. We expect that if lower leakage devices become available, we would be able to measure noise temperatures in the $3 \, h\nu/k$ range even with a 4.2 K helium bath.

In figure 7, plot the receiver noise temperature as a function of LO frequency for different bias conditions and different helium bath temperatures. Low noise operation is achieved up to 714 GHz, the highest frequency of our LO unit. Measurements with Fourier Transform Spectrometer indicate that the receiver should have reasonable performance up to 730 GHz.

In Fig. 8 we display frequency dependence of the sensitivity of 3 different mixers in our test receiver. The 0.60 x 23 μm resonator has a noise temperature below 200 K between 580 and 690 GHz, corresponding to a bandwidth of about 17%. These data shows that the frequency response of these resonant mixers is controlled mostly by the width of the resonator, rather than by the length. For example, the 0.60 x 23 μm resonator is centered at a

lower frequency than the $0.55 \times 25 \mu\text{m}$ resonator. This is consistent with the results of the calculations shown in Fig. 3.

V. IF Bandwidth

One concern about distributed SIS mixers is their large geometrical capacitance which may limit the useful IF bandwidth. For example, in the $0.55 \times 25 \mu\text{m}$ resonator, the device capacitance is estimated to be about 0.9 pF, considerably higher than other lumped element designs, which typically have a total of 0.3 pF output capacitance [6,9,10]. We have made detailed measurement of the IF performance of our mixer using a 2 – 4 GHz amplifier and a 4 – 8 GHz amplifier. The noise temperature of both amplifiers is in the 3 – 4 K range and we incorporate a circulator cooled to 4.2 K between the mixer and IF amplifier. The measured data is summarized in Fig. 9.

The data confirms that the receiver performance degrades with increasing IF. Using a single pole roll-off model, we derive a 3-dB IF bandwidth of 6 GHz from the experimental data. At an IF of 6 GHz, the conversion loss is about -9 dB versus -7 dB at around 3 GHz, and the noise temperature is 170 K versus 140 K at 3 GHz. From the sensitivity point of view, this mixer will be useful up to an IF frequency of 8 GHz, at which point, the noise temperature is about 1.4 times the noise temperature at lower IF, which corresponds to a doubling of integration time needed to obtain the same signal-to-noise ratio when a faint signal is being received.

The IF roll-off can be understood by considering the equivalent output circuit of the mixer as shown in Fig. 10. In this circuit, R_{out} is the output resistance of the

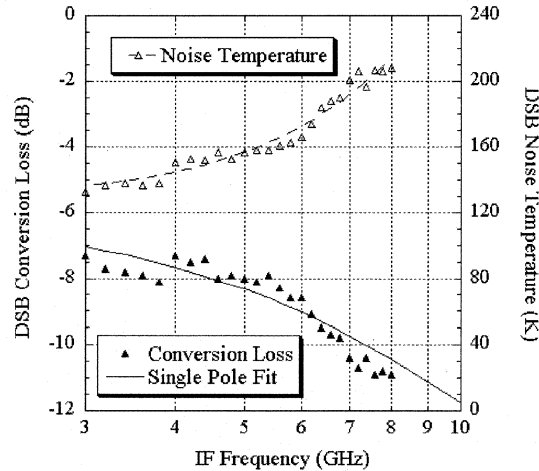


Fig. 9 IF Response of a $0.55 \times 25 \mu\text{m}$ resonator. The conversion loss data has been fitted with a single pole roll-off model that has a 3-dB roll-off at about 6 GHz.

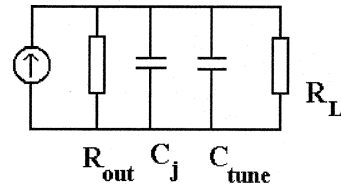


Fig. 10 Equivalent Output Circuit of SIS Mixer

device given by dV/dI on the current-voltage characteristic of the device in the presence of LO drive. C_j is the junction capacitance and C_{tune} is any parasitic capacitance introduced by any matching circuit. In the case of the resonant mixer, C_{tune} is introduced by the transformer section and it is much smaller than C_j . Assuming that the mixer output is connected to a constant load, R_L , the 3-dB IF bandwidth as a result of this RC circuit can simply be written as:

$$F_{3\text{-dB}} = \frac{R_{\text{out}} + R_L}{2\pi \cdot R_{\text{out}} \cdot R_L \cdot (C_j + C_{\text{tune}})} = \frac{(1 + \frac{R_{\text{out}}}{R_L})}{2\pi \cdot r \cdot (R_N A) \cdot (1 + \chi) C_{\text{sp}}} \quad (7)$$

where $r = R_{\text{out}}/R_N$ and $\chi = C_{\text{tune}}/C_j$. In our mixer, $R_L = 50 \Omega$, $R_{\text{out}} \sim 45 \Omega$ and $\chi \ll 1$, and we have $F_{3\text{-dB}} \sim 7.5$ GHz. This is close to the fitted value of 6 GHz.

It is clear from equation (7) that when $R_{\text{out}} \sim R_L$, the IF bandwidth limitation is imposed not so much by the large junction capacitance but by a large value of r , the ratio between the output resistance and the normal-state resistance. In this example, we have $r > 10$. However, this seems unavoidable at high operating frequency where the quasi-particle tunneling step is very wide and the step is more likely to be flat, giving rise to relatively high values of R_{out} . This does not seem to be unique to resonant mixers. We also note that the IF bandwidth depends on the $R_N A$ product. Clearly, we may improve the IF bandwidth by increasing the current density of the tunnel junction. However, at higher current density, C_{sp} slowly increases, so that the gain in bandwidth may be limited.

Equation (7) can be applied to all other types of SIS mixers. In many lumped element mixer designs, the tuning circuit may involve a large capacitance, making $\chi > 1$, in which case, equation (7) predicts that the IF bandwidth will be smaller than resonant mixers.

The above discussion assumes a constant IF load. An IF matching circuit can always be designed to reduce the impact of the IF roll-off effect. The large geometrical capacitance of the distributed mixer does not seem to impose a fundamental limit on the IF bandwidth of the mixer.

VI. Conclusion

A near Quantum-limited sensitivity has been achieved in the 600 – 720 GHz frequency band using an SIS resonant mixer receiver. The tunnel junction resonators in our mixer design can be modeled easily through a simple linear transmission line equations. Using transformer-coupled full wave Nb/AlN/Nb resonators, we have measured noise

temperatures as low as 141 K at 700 GHz with the mixer cooled to 4.2 K and 111 K with the mixer cooled to 2.8 K. The mixers exhibit a 17% RF bandwidth, have a measured 3-dB IF bandwidth of 6 GHz and useful sensitivities up to an IF bandwidth of about 8 GHz.

References

- [1] C.E. Tong, R. Blundell, B. Bumble, J.A. Stern, and H.G. LeDuc, "Quantum-limited heterodyne detection in superconducting nonlinear transmission lines at sub-millimeter wavelengths," *Appl. Phys. Lett.*, vol. 67, pp. 1304-1306, Aug. 1995.
- [2] C.E. Tong, L. Chen, and R. Blundell, "Theory of distributed mixing and amplification in a superconducting quasi-particle nonlinear transmission line," *IEEE Trans. Microwave Theory Tech.*, vol. 45, pp. 1086-1092, July 1997.
- [3] Y.V. Belitsky, and E.L. Kollberg, "Superconductor-insulator-superconductor tunnel strip line," *J. Appl. Phys.*, vol. 80, pp. 4741-4748, 1996.
- [4] Y. Uzawa, A. Kawakami, S. Miki, and Z. Wang, "Performance of all-NbN quasi-optical SIS mixers for the terahertz-band," *IEEE Trans. Appl. Supercond.*, vol. 11, pp. 183-186, 2001.
- [5] T. Matsunaga, C.E. Tong, T. Noguchi, R. Blundell, "Fabrication and characterization of a 600 GHz resonant distributed SIS junction for fixed-tuned waveguide receiver," *Proc. 12th Int. Symp. Space THz Tech.*, pp. 571-580, I. Mehdi, ed, San Diego, CA, Feb. 2001.
- [6] C.E. Tong, R. Blundell, S. Paine, D.C. Papa, J. Kawamura, X. Zhang, J.A. Stern, and H.G. LeDuc, "Design and characterization of a 250-350 GHz fixed-tuned Superconductor-Insulator-Superconductor receiver," *IEEE Trans. Microwave Theory Tech.*, vol. 44, pp. 1548-1556, Sept. 1996.
- [7] D.C. Mattis, and J. Bardeen, "Theory of the anomalous skin effect in normal and superconducting metals," *Phys. Rev.*, vol. 111, pp. 412- 418, July 1958.
- [8] J.R. Tucker, and M.J. Feldman, "Quantum detection at millimeter wavelengths," *Rev. Mod. Phys.*, vol. 57, pp. 1055-1113, Oct. 1985.
- [9] R. Blundell, C.E. Tong, D.C. Papa, R.L. Leombruno, X. Zhang, S. Paine, J.A. Stern, and H.G. LeDuc, "A wideband fixed-tuned SIS receiver for 200 GHz operations," *IEEE Trans. Microwave Theory Tech.*, vol. 43, pp. 933-937, 1995.
- [10] C.E. Tong, R. Blundell, D.C. Papa, J.W. Barrett, S. Paine, X. Zhang, J.A. Stern, and H.G. LeDuc, "A fixed-tuned low noise SIS receiver for the 600 GHz frequency band," *Proc. 6th Int. Symp. Space THz Tech.*, pp. 295-304, J. Zmuidzinas, ed, Pasadena, CA, Mar. 1995.
- [11] J. Kawamura, R. Blundell, C.E. Tong, D.C. Papa, T.R. Hunter, S.N. Paine, F. Patt, G. Gol'tsman, S. Cherednichenko, B. Voronov, and E. Gershenzon, "Superconductive hot-electron-bolometer mixer receiver for 800 GHz operation," *IEEE Trans. Microwave Theory Tech.*, vol. 48, pp. 683-689, 2000.